

Lawrence Berkeley National Laboratory

LBL Publications

Title

LOW-ENERGY ELECTRON DIFFRACTION, AUGER ELECTRON SPECTROSCOPY, and THERMAL DESORPTION STUDIES OF CHEMISORBED CO and O₂ ON THE (111) and STEPPED [6(111)x(100)] IRIDIUM SURFACES

Permalink

<https://escholarship.org/uc/item/2c95r2j1>

Author

Hagen, D.I.

Publication Date

1975-11-01

0 0 0 4 4 0 7 0 3 8

Submitted to Surface Science

LBL-4527
Preprint c. |

LOW-ENERGY ELECTRON DIFFRACTION, AUGER ELECTRON
SPECTROSCOPY, AND THERMAL DESORPTION STUDIES OF
CHEMISORBED CO AND O₂ ON THE (111) AND STEPPED
[6(111)x(100)] IRIDIUM SURFACES

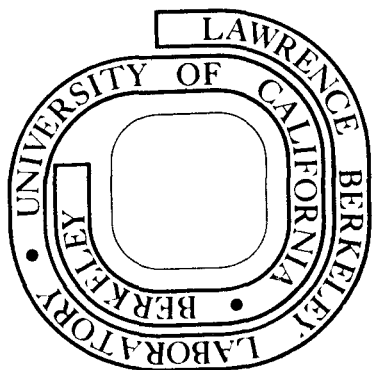
D. I. Hagen, B. E. Nieuwenhuys, G. Rovidia, and
G. A. Somorjai

November 1975

Prepared for the U. S. Energy Research and
Development Administration under Contract W-7405-ENG-48

For Reference

Not to be taken from this room



LBL-4527
c. |

DISCLAIMER

This document was prepared as an account of work sponsored by the United States Government. While this document is believed to contain correct information, neither the United States Government nor any agency thereof, nor the Regents of the University of California, nor any of their employees, makes any warranty, express or implied, or assumes any legal responsibility for the accuracy, completeness, or usefulness of any information, apparatus, product, or process disclosed, or represents that its use would not infringe privately owned rights. Reference herein to any specific commercial product, process, or service by its trade name, trademark, manufacturer, or otherwise, does not necessarily constitute or imply its endorsement, recommendation, or favoring by the United States Government or any agency thereof, or the Regents of the University of California. The views and opinions of authors expressed herein do not necessarily state or reflect those of the United States Government or any agency thereof or the Regents of the University of California.

Low-Energy Electron Diffraction, Auger Electron Spectroscopy, and Thermal
Desorption Studies of Chemisorbed CO and O₂ on the (111) and
Stepped [6(111)×(100)] Iridium Surfaces

by

D. I. Hagen,^{*} B. E. Nieuwenhuys,^{**} G. Rovida,⁺ and G. A. Somorjai

Materials and Molecular Research Division, Lawrence Berkeley Laboratory,
and Department of Chemistry, University of California,
Berkeley, California 94720

ABSTRACT

The adsorption of CO, O₂, and H₂O was studied on both (111) and [6(111)×(100)] crystal faces of iridium. The techniques used are LEED, AES, and thermal desorption. Marked differences were found in surface structures and heats of adsorption on these crystal faces. Oxygen is adsorbed in a single bond state on the (111) face. On the stepped iridium surface an additional bonding state with a higher heat of adsorption was detected which can be attributed to oxygen adsorbed at steps. On both (111) and stepped iridium crystal faces the adsorption of oxygen at room temperature produced a (2×1) surface structure. Three surface structures were found for CO adsorbed on Ir(111); a ($\sqrt{3}\times\sqrt{3}$)R 30° at an exposure of 1.5-2.5 L and a ($2\sqrt{3}\times 2\sqrt{3}$)R 30° at higher coverage. No indication for the ordering of adsorbed CO was found on the Ir(S)-[6(111)×(100)] surface. No significant differences in thermal desorption spectra of CO were found on these two faces. H₂O is not adsorbed at 300 K on either iridium crystal face. The reaction of CO with O₂ was studied on Ir(111) and the results are discussed. The influence of steps on the adsorption behaviour of CO and O₂ on iridium and the correlation with the results found previously on the same platinum crystal faces are discussed.

* Presently at: Union Carbide Laboratories, South Charleston, West Virginia.

** Permanent address: Gorlaeus Laboratoria, Leiden. The Netherlands.

+ Permanent address: Istituto di Chimica Fisica, Università di Firenze, Italy.

Introduction

One of the most fruitful approaches to the understanding of the nature of chemical bonding is the systematic investigation of how physical-chemical properties vary for elements across the periodic table. The correlation of chemisorption characteristics of gases on transition metal surfaces for this purpose is an important but difficult task for several reasons. The adsorption behaviour varies markedly from crystal face to crystal face. Ordering in the adsorbed layer that can be detected by low-energy electron diffraction (LEED), the degree of dissociation of the adsorbates on the surface, the strength of bonding in both dissociated and undissociated states can all vary markedly with crystallographic orientation and also with surface cleanliness. Experimental techniques, however, are available to study ordering and bonding on crystal surfaces as a function of orientation while making sure that the surface is clean.

We have studied the chemisorption of CO and O₂ on two types of iridium surfaces, one with low Miller Index (111) and one with high Miller Index (775) (or stepped [6(111)×(100)]) by a combination of techniques that include LEED, Auger Electron Spectroscopy (AES), flash desorption and mass spectroscopy. In a subsequent paper the chemisorption behaviour of hydrogen and various hydrocarbons on the same two crystal faces of iridium will be reported.

Iridium is the nearest neighbor of platinum in the periodic table whose chemisorption characteristics have been investigated in detail. It was found¹⁾ that the adsorption behaviour of platinum is very sensitive to the presence of steps present on the surface in large concentrations that is characteristic of high Miller Index surface structures. Ordering in the adsorbed layer was much poorer, molecules were dissociating readily and

the heats of adsorption appeared to be higher on stepped platinum surfaces. Theories have been proposed²⁾ to explain the different chemical bonding at irregularities (steps, kinks) on the surfaces of transition metals in terms of local charge density redistribution and altered crystal field splitting at these surface sites. The theory also predicted that charge density redistribution at steps that result in the altered chemical behaviour is limited to metals with large density of states at the Fermi level like platinum, iridium, and most transition metals. This prediction was borne out by our chemisorption studies on (111) and stepped [6(111)×(100)] gold surfaces.³⁾ This metal has low density of states at the Fermi level and has shown identical chemisorption behaviour for low Index (111) and stepped surfaces within the accuracy of the experiment.

We have thus turned our attention to the chemisorption behaviour of iridium low Miller Index and stepped surfaces to uncover what effect, if any, the surface irregularities have on the adsorption characteristics of this metal, and to compare them with that of platinum. We have found that the surface structures and bonding are markedly different on stepped iridium surfaces when compared to the iridium (111) crystal face as expected from theoretical considerations as well. We have also found differences in the ordering characteristics of iridium and platinum surfaces of the same structure that indicate a stronger metal-adsorbate bond and greater barrier to mobility of adsorbates on the iridium metal surface.

Experimental

The two iridium samples were cut from a single crystal of 99.99% nominal purity from Materials Research Corporation. The main impurities were Ru (100 ppm), W (40 ppm), Pt (30 ppm), and Fe(15 ppm), other impurities being at concentrations less than 10 ppm. The samples were cut within 1° of the desired orientation, and their surfaces polished and etched before installation in the vacuum chamber. The surface area of the edges of the crystals that are of random surface structure is about 10 and 20% of the total surface area ($\sim 1 \text{ cm}^2$) for the (111) and the stepped plane, respectively.

Two separate LEED-Augur apparatus were employed in these studies, both with four-grid electron optics and equipped with a quadrupole mass spectrometer. In both systems typical residual pressures of 1×10^{-9} Torr were obtained.

The temperature of the samples was measured by means of thermocouples spot welded near the edge of the crystals. Measurements made with infrared and optical pyrometers indicated that the difference in temperature across the surface of the samples was not more than about 5%, even during rapidly increasing temperature during flash desorption.

The main surface impurity was found to be carbon that could be removed by heating crystals to 500-600°C in an oxygen ambient at 5×10^{-7} Torr for several minutes followed by flashing to 1200°C to remove surface oxygen. Small amounts of sulfur were easily removed by a similar treatment. Following this treatment, no surface impurity was found within the limits of sensitivity of AES.

Results

A. The Clean Ir(111) and Ir-[6(111)×(100)] Surfaces

Following cleaning, the Ir(111) surface gave the characteristic hexagonal (1×1) LEED diffraction pattern as shown in Fig. 1a and the Ir(S)-[6(111)×(100)] gave the expected pattern with the (1×1) spots split in the direction perpendicular to the steps, as shown in Fig. 10a. The structure of the stepped surface was found to be completely stable in vacuum to temperatures as high as 1200°C.

B. Interaction of CO with the Ir(111) Surface

Exposure of the clean surface at room temperature or -50°C to CO initially yields a diffraction pattern corresponding to the $(\sqrt{3}\times\sqrt{3})R\ 30^\circ$ surface structure as shown in Fig. 1b. This structure, observed previously by Grant,⁴⁾ is first detectable at an exposure of about 1.5 L (1 L = 1 Langmuir = 10^{-6} Torr sec) and becomes fully developed at an exposure of about 2.5 L. The adsorption was carried out in the pressure range of 5×10^{-9} to 5×10^{-7} Torr and there was no apparent dependence of the ordering behaviour on CO pressure. As the exposure is continued, the extra diffraction spots became less intense and diffuse and they are observed to split.

At higher exposures, the split diffuse spots become sharper again and the new diffraction pattern that develops indicates the formation of a $(2\sqrt{3}\times 2\sqrt{3})R\ 30^\circ$ surface structure as shown in Fig. 1c & d. This structure is observed as the surface becomes saturated with CO for exposures >25 L. The extra diffraction spots, characteristic of this structure, are more distinct when adsorption is carried out at -50°C instead of 25°C. If part of the CO is desorbed from the surface by heating the $(\sqrt{3}\times\sqrt{3})R\ 30^\circ$ structure is again obtained. The formation of the $(2\sqrt{3}\times 2\sqrt{3})R\ 30^\circ$ structure is not due to an interaction of the electron beam with the surface. However, prolonged exposure of the

$(2\sqrt{3} \times 2\sqrt{3})R 30^\circ$ structure to the electron beam would result in the spots becoming more diffuse.

The high coverage structure can be understood to arise from the $(\sqrt{3} \times \sqrt{3})R 30^\circ$ surface structure by a compression of the adsorbate layer in the way as shown in Fig. 2. Three domains of the coincidence lattice of this compressed layer (shown in Fig. 2b) rotated 120° can explain the observed $(2\sqrt{3} \times 2\sqrt{3})R 30^\circ$ structure. This is thought to be the most likely model because it corresponds to a coverage of 1.0×10^{15} molecules/cm², or $2/3$ monolayer, as was found experimentally. The proposed structure is similar, but more compressed than that found by Conrad et al.⁵⁾ at saturation on Pd(111). The shortest CO-CO distance is 3.1 \AA which is compatible with the dimension of the adsorbed CO molecule as found on other metals.^{5,6)}

Typical thermal desorption curves for CO on Ir(111) are shown in Fig. 3. These were obtained after exposing the clean surface to a given exposure of CO by flashing the surface in vacuum. The CO partial pressure was recorded as a function of time during the flash and yields the curves shown in Fig. 4. Because of the high pumping speed of the system, the area under each curve is proportional to the initial coverage obtained from the given exposure. The amount of CO adsorbed that is measured in this way as a function of exposure is shown in Fig. 4. Also included in the figure are the carbon Auger peak heights, due to adsorbed CO, as a function of exposure. The Auger results are normalized to the thermal desorption results at saturation, that is, at exposures higher than those shown in the plot. Also shown is the amount corresponding to a coverage of $\theta = 1/3$ obtained by assuming the well-developed $(\sqrt{3} \times \sqrt{3})R 30^\circ$ structure (at 2.5 L) corresponds to a coverage of $1/3$ or 5.2×10^{14} molecules/cm². The saturation coverage is then seen to be near to $2/3$, as discussed above.

An independent calculation of the amount adsorbed was made by estimating the system volume, CO pumping speed, and sample area. A value of 4.7×10^{14} molecules/cm² was then found to correspond to an exposure of 2.5 L, in good agreement with the value of 5.2×10^{14} molecules/cm² for a coverage of 1/3. Figure 4 also shows that the carbon Auger peak height is directly proportional to coverage as determined by thermal desorption over the entire coverage range. The heights of the Auger carbon and oxygen peaks due to adsorbed CO were always found to change in an identical manner and in proportion with the amount of adsorbate.

As seen in Figure 4, the sticking probability for CO on Ir(111) is constant (0.6) up to an exposure of about 2.0 L where the $(\sqrt{3} \times \sqrt{3})R 30^\circ$ structure is well-developed. Following the formation of this structure, the sticking probability decreases rapidly to 0.04 and remains almost constant during the formation of the $(2\sqrt{3} \times 2\sqrt{3})R 30^\circ$ superstructure.

As shown in Fig. 3, the thermal desorption spectra for CO consists only of a single peak at low exposures and an additional peak at a slightly lower temperature at high exposures. The low temperature peak is not evident in the flash desorption spectra that is associated with the presence of the $(\sqrt{3} \times \sqrt{3})R 30^\circ$ surface structure. There is also a small high temperature shoulder present on all the CO spectra. This shoulder was not observed if the surface was contaminated with carbon. The temperature at which the low exposure thermal desorption peak appears was found to decrease slightly for increasing coverage. This is probably due to the decreasing heat of desorption with increasing coverage for the first order CO desorption, rather than indicative of second order desorption kinetics. The low exposure thermal desorption peak was also found to occur at a significantly

lower temperature if carbon contamination was present on the surface.

The heat of adsorption was obtained from the reversible behaviour of the LEED pattern corresponding to the $(\sqrt{3}\times\sqrt{3})R 30^\circ$ structure. For a given CO pressure the sample temperature was changed until the $(\sqrt{3}\times\sqrt{3})R 30^\circ$ structure was just observed. This was repeated for several different CO pressures yielding the results shown in Fig. 5. The least-square straight line drawn through the points in the figure may be considered as an isostere at a coverage of about 1/3 monolayer and whose slope yields the isosteric heat of adsorption of 39 ± 3 kcal/mole. This value is near to the 37 kcal/mole found by Christmann and Ertl for CO on Ir(110) face.⁷⁾

On the Ir(111) surface all adsorbed CO could be removed from the surface by "flashing" as evidenced by the lack of any residual carbon Auger peak following desorption. No evidence for thermal decomposition of CO on the Ir(111) surface was found for temperatures below 500°C. This is in contrast to the Ir(110) surface where dissociation of CO was found to take place above 200°C.⁷⁾ However, when the surface was held at $T > 500^\circ\text{C}$ and exposed to CO for a long time, a small carbon Auger peak was found suggesting dissociation. Possible contamination by reaction with small amounts of hydrocarbons in the ambient cannot, however, be excluded. Electron beam induced dissociation is a potential problem with adsorbed CO. In our study some evidence for desorption and dissociation under the electron beam was found. Such effects were minimized by employing a defocused Auger primary beam and reducing LEED observation times.

The Auger peak shape associated with CO adsorbed on iridium is shown in Fig. 6. In the figure it is also shown for comparison an Auger spectrum corresponding to an Ir surface partly contaminated by amorphous carbon. As

far as we know, similar Auger double peaks for C have not been detected for CO adsorbed on other metal structures. The observed double peak for CO was observed on the stepped surface as well as on the (111) surface. Since the stepped surface studies and the (111) studies were carried-out in different experimental systems, the double peak shape cannot be explained as an experimental artifact.

C. Interaction of CO with the Ir(S)-[6(111)×(100)] Surface

In contrast to the (111) surface no ordered LEED structures were observed as a consequence of CO adsorption on the stepped surface up to exposures of several hundred L. Only an increased background was observed following adsorption, superimposed on the normal Ir(S)-[6(111)×(100)] diffraction pattern.

Thermal desorption spectra for this surface were found to be similar to that of the Ir(111) surface (Fig. 3) with desorption maximum in the range 240-280°C, decreasing with increasing coverage. As with Ir(111), evidence was found for an additional low temperature peak at high coverages but only poorly resolved. A small high temperature shoulder, superimposed on the thermal desorption spectra from the stepped surface, was also present as was also observed on the (111) surface.

No evidence for thermal dissociation of CO was found on the stepped surface up to at least 500°C in agreement with the behaviour of the Ir(111) surface. Some dissociation of adsorbed CO was observed in the presence of the Auger electron beam particularly in the presence of a CO ambient. The Auger beam also caused electron impact desorption of adsorbed CO.

D. Interaction of O₂ with the Ir(111) Surface

The adsorption of O₂ on the Ir(111) surface was found to produce extra spots in the LEED diffraction pattern superimposed on the clean Ir(111)-(1x1) pattern. At adsorption pressures of 5×10^{-8} to 5×10^{-7} Torr and with the sample at room temperature half-order extra spots were first observed at an exposure of about 10 L. Initially the spots were found to be elongated as shown in Fig. 7a. This behaviour suggests that the surface layer consists of domains of a (2x1) structure with disorder in the direction of the shorter unit cell vector. At an exposure of about 30 L the spots become round and sharp indicating the formation of an apparent (2x1) or (2x2) structure as shown in Fig. 7b. No further changes are observed in the diffraction pattern for exposures as high as 150 L. These observations suggest the saturation coverage for O₂ on Ir(111) is 0.5 monolayer corresponding to a (2x1) structure. The same surface structure designated as an Ir(111)-(2x2)-0 structure has been reported by Grant.⁴⁾ The extra spots indicative of the (2x1)-0 surface structure were found to become diffuse on heating the surface above 100°C and to disappear almost entirely on heating to 200-400°C following exposure to oxygen. On recooling the sample, following this treatment, the extra spots would reappear. If cooling the iridium crystal was carried-out in vacuum, the reappearance of the diffraction pattern was slow and yielded only diffuse spots. Cooling in an O₂ ambient (5×10^{-7} Torr) the diffraction pattern appeared more rapidly with the final formation of sharp spots as observed prior to heating.

Thermal desorption spectra for O₂ adsorbed on Ir(111), obtained in an analogous fashion to adsorbed CO on Ir(111), are shown in Fig. 8. As seen in the figure, only a single broad peak is present. The temperature of the

peak is found to decrease strongly over a range of 620-850°C with increasing coverage, suggesting second order desorption kinetics.

The amount of O₂ adsorbed at room temperature on a clean Ir(111) surface as a function of exposure derived from thermal desorption is shown in Fig. 9. Also included in Fig. 9 are the oxygen Auger peak heights as a function of exposure. An adsorption pressure of 10⁻⁷ Torr was employed to obtain the thermal desorption data in Fig. 9 and a pressure of 5 × 10⁻⁸ Torr was used to obtain the Auger spectrum. The adsorption of O₂ on Ir(111), as well as CO on Ir(111), depends only on exposure in the pressure range 10⁻⁸ to 10⁻⁶ Torr. As seen in Fig. 9, saturation is reached at an exposure of about 30 L. Assuming a saturation coverage of 0.5 monolayer, and the dissociation of oxygen molecules on adsorption, an initial sticking probability of 0.05 is deduced. Both the desorption temperature and the sticking probability found in this work for chemisorbed oxygen on Ir(111) surface are in agreement with the β₁ phase reported by Ageev and Ionov for a polycrystalline iridium strip.⁸⁾ We had no evidence for the presence on Ir(111) of a higher binding state corresponding to the β₂ phase found by these authors. The maximum amount of adsorbed oxygen as found by Ageev and Ionov⁸⁾ corresponds roughly to 1/2 monolayer on a (111) plane, in agreement with a (2×1) surface structure as assumed in the present study.

No evidence was found for the formation of bulk iridium oxide upon exposure to oxygen, even at temperatures of 600°C and pressures of 10⁻⁶ Torr. The rate of formation of IrO₂ has been found to be detectable at higher oxygen pressures.⁹⁾

E. Interaction of O₂ with the Ir(S)-[6(111)×(100)] Surface

Adsorption of oxygen on the stepped surface at room temperature produced a diffraction pattern, shown in Fig. 10b, consisting of the clean Ir(S)-[6(111)×(100)] pattern with split half-order extra spots consistent with a (2×2) surface structure. Heating this surface to about 200°C resulted in a diffraction pattern characteristic of a (2×1) surface structure and is shown in Fig. 10c. The extra spots in the diffraction pattern were split and the initial presence of streaks, as shown in the figure, was observed. The (2×1) structure was found to be stable up to 450°C. Cooling to room temperature in an O₂ ambient does not restore the (2×2) pattern. Further heating to about 450°C in 10⁻⁷ Torr O₂ resulted in the disappearance of the (2×1) structure. The doublets become diffuse and elongated as shown in Fig. 10d indicating alterations of the step periodicity. The results may be interpreted by considering that three domains of (2×1) are formed at room temperature, simulating a (2×2) structure. On heating, the mobility of the atoms increases and the orientation of the steps favours the formation of that particular (2×1) domain which has the most densely packed rows parallel to the steps.

The thermal desorption spectra (shown in Fig. 11) exhibits two desorption peaks, one with a maximum near 800°C and the other near 1200°C. The lower binding energy state, observed at higher exposures is the same as that found on the (111) crystal. The second peak, appearing first at low exposures, was not observed on the (111) crystal. This peak can be interpreted as due to a higher binding state of the oxygen atoms adsorbed at the steps. The high temperature peak can be related to the β₂ phase reported by Ageev and Ionov⁸⁾ on polycrystalline iridium.

F. Reaction of CO with O₂ on Ir(111)

In order to determine the dependence of the rate of CO₂ formation on temperature, the clean Ir(111) surface was exposed to a 1:1 mixture of CO and O₂ at a total pressure held constant at 2×10^{-7} Torr. The partial pressure of CO₂ was then monitored with the mass spectrometer while the sample temperature was changed step-wise. Figure 12 shows the CO₂ pressure as a function of sample temperature under these conditions. In our experimental conditions the increase in the CO₂ pressure is proportional to the reaction rate. The figure shows that the reaction rate has a maximum at 300°C.

Although it was not possible to observe LEED structures during the reaction as a function of temperature, LEED observations at room temperature concerning the interaction of O₂ with CO on the Ir(111) surface are described below.

The LEED pattern that is observed following exposure of the clean Ir(111) surface to a mixture of O₂ and CO depends on the ratio of these gases. For CO:O₂ \geq 1:2, at a total pressure of 1×10^{-7} Torr, mainly CO adsorption takes place as evidenced by the formation of $(\sqrt{3} \times \sqrt{3})R 30^\circ$ and $(2\sqrt{3} \times 2\sqrt{3})R 30^\circ$ structures and the presence in the thermal desorption spectra of only a CO peak. Exposure to CO:O₂ \approx 1:5, at a total pressure of 1×10^{-7} Torr, results in the formation of a (2 \times 2) surface structure. This structure is attributed to a mixed adsorbate, consisting of both CO and oxygen, for the following reasons. The half-order diffraction spots were found to be circular and diffuse in the early stages of the development of the diffraction pattern in contrast to the elongated spots observed in the formation of the (2 \times 1)-0

surface structure. This suggests the formation of a true (2×2) surface structure for the mixture. The intensities of the half-order spots were observed to vary with beam voltage in a different way as compared to pure oxygen adsorption. Also, the thermal desorption spectra showed mainly a large CO₂ peak with only small contributions from CO and O₂ depending on the gas composition during adsorption. The ratio between O atoms and CO molecules in this mixed surface phase has not been evaluated. A possible arrangement of O and CO on the surface, giving the observed (2×2) structure, is a superposition of a (2×2)-O mesh on a (2×2)-CO mesh shifted by half the diagonal so that a CO molecule is located at the center of the O cell or vice versa. This structure would explain why the half-order spots remain circular during adsorption since there are no preferred directions for ordering. When the CO pressure is a few percent of that of O₂, the (2×1)-O is formed, and mostly O₂ is desorbed with a few percent of CO₂.

Exposing the clean surface at room temperature to the two gases, O₂ and CO, sequentially at 10⁻⁷ Torr was found to give the LEED structure appropriate to the first gas incident on the surface. Changes in the diffraction pattern were observed on admission of the second gas (after pumping out the first gas), but they occurred very slowly. It was observed that CO was very slowly being replaced from the surface by O₂ much more slowly than the replacement of O₂ by CO. Considerable caution had to be exercised in the use of LEED to study the CO adsorbate in the presence of O₂ in the gas phase. It was found that a (2×2) structure rapidly began to grow at the expense of the CO structure. On shifting the LEED beam to a new location on the sample, however, the initial CO structure was observed. Thermal desorption indicated only the presence of adsorbed CO.

G. Interaction of H₂O with Ir(111) and Ir(S)-[6(111)×(100)]

Adsorption of H₂O could not be detected at room temperature and pressure up to 10⁻⁷ Torr both on the (111) and the stepped crystal plane.

DISCUSSION

The results of CO adsorption indicate marked difference in chemisorption characteristics for the (111) and the stepped iridium surfaces, respectively. While two ordered surface structures form on the (111) crystal face, $(\sqrt{3}\times\sqrt{3})R\ 30^\circ$ and $(2\sqrt{3}\times 2\sqrt{3})R\ 30^\circ$, with increasing coverage, ordering of the adsorbed CO was not observed on the stepped surface. It appears that the steps effectively prevented ordering or the formation of large enough ordered domains of the adsorbate to be detectable by LEED. Bonding characteristics of CO as judged from the flash desorption studies and from the apparent absence of dissociation of the adsorbate are similar on both crystal faces. As in the case of platinum, the (100) orientation step atoms cannot dissociate the high binding energy CO molecule in our experimental conditions without the help of the electron beam.

Oxygen was found to order on both (111) and stepped iridium surfaces. From the flash desorption characteristics it appears that oxygen is bound more strongly at the steps than on the (111) face. It is interesting to note that Conrad et al. has found similar bonding behaviour on comparing the chemisorption characteristics of hydrogen¹⁰⁾ and CO⁵⁾ on the (111) and Pd[9(111) \times (111)] stepped palladium surfaces. While the initial heat of adsorption of hydrogen was higher on the stepped surface, the heat of CO adsorption was the same for both surfaces.

Water was found not to adsorb on either iridium surface at room temperature.

The co-adsorption behaviour of CO and O₂ is that expected from the relative sticking probabilities. The virtually unchanged sticking probability of CO while the $(\sqrt{3}\times\sqrt{3})R\ 30^\circ$ surface structure is formed and the marked

decrease of the sticking probability as the $(2\sqrt{3}\times 2\sqrt{3})R\ 30^\circ$ structure forms along with the ordered oxygen adsorption and co-adsorption make this system an excellent choice for thermodynamic studies in the adsorbate layer.

The reaction rate for oxidation of CO, measured on the (111) face shows a temperature dependence similar to that found by Christman and Ertl⁷⁾ on Ir(110), indicating that this reaction has the same mechanism on both faces, despite the differences in surface structure.

It is of value to compare the chemisorption behaviour of the different gases on platinum and iridium (111) and stepped $[6(111)\times(100)]$ surfaces. Table I lists the ordering characteristics of those systems. CO forms ordered structures on the (111) surfaces of both metals, but the structures appear to be different. On the stepped surfaces of both metals, CO remains disordered. It is difficult to determine with any degree of certainty whether some of the adsorbed CO dissociates on these high Miller Index surfaces, due to the presence of electron beams in all of these experiments. It is clear that only a small fraction of the adsorbed CO monolayer may dissociate, if any, as judged by AES studies and thermal desorption spectra.

Oxygen appears to order well on iridium surfaces. There is some degree of uncertainty about adsorption of oxygen on Pt(111).¹²⁾ When O_2 has been observed to adsorb in an ordered manner on Pt(111) a (2×2) surface structure has been found,¹²⁾ similar to that on Ir(111). Although bonding energies would be expected to be greater on iridium than on platinum, there is no direct evidence for the formation of iridium-oxide on the (111) stepped surface. On the other hand, surface oxides of platinum¹¹⁾ and even of gold³⁾ have been detected under conditions of oxygen exposure and surface temperatures used in this study. It is possible to relate the periodicity

of the Ir(2×1)-O structure to that of IrO₂(100) plane which has been observed as the dominant surface orientation during the growth of IrO₂ on Ir(111).⁹⁾ The distances between the oxygen atoms in the (2×1)-O structure (2.7 and 4.7 Å) are near to those in the (100) plane of the oxide (3.1 and 4.5 Å).¹³⁾

The heat of adsorption of CO is higher on Ir(111) than on Pt(111).¹⁴⁾ It is interesting to note that also the temperature, where the rate of CO₂ formation from CO and O₂ mixtures increases strongly, appears to be higher on Ir(111) than on Pt(111).¹⁵⁾ These temperatures (around 170°C on Pt(111) and around 225°C on Ir(111)) are equal to the temperatures where desorption of CO may be expected under the experimental conditions used in these experiments. The occurrence of the sudden increase in reaction rate can, therefore, be attributed to desorption of CO from the surface.

The differences in the chemisorption behaviour (surface structure, bonding) of these two gases are marked between (111) and stepped surfaces of the same metal. These observations, that are confirmed in studies of hydrocarbon chemisorption that will be reported in a subsequent paper, underline the surface structure sensitivity of chemisorption. Chemisorption studies on polycrystalline surfaces of metals may not, in most cases, be comparable with chemisorption studies on single crystal surfaces, for this reason.

The differences in chemisorption characteristics between the two metal surfaces, platinum and iridium, of the same surface structure indicate that localized bonding of the adsorbate to the individual surface atoms is just as important in forming the surface chemical bond as that of the atomic surface structure.

Acknowledgment:

This work was supported by the U. S. Energy Research and Development Administration and the Office of Naval Research (N00014-75-C-0890).

Table I. Comparison of Structures Observed on (111) and Stepped Surfaces of Ir and Pt

Adsorbate	Substrate			
	Ir(111)	Ir(S)-[6(111)×(100)]	Pt(111)	Pt(S)-[6(111)×(100)]
CO	$(\sqrt{3}\times\sqrt{3})R30^\circ$ $(2\sqrt{3}\times2\sqrt{3})R30^\circ$	disordered	$(4\times2)^{11)}$ $(2\times2)^{11)}$	disordered ¹¹⁾
O ₂ (25°C)	(2×1)	(2×1)	not adsorbed ¹¹⁾ $(2\times2)^{12)}$	2(1d) ¹¹⁾
H ₂ O	not adsorbed	not adsorbed	not adsorbed ³⁾	not adsorbed ³⁾

REFERENCES

1. G. A. Somorjai, R. W. Joyner, and B. Lang, Proc. Roy. Soc., London A, 331, 335 (1972).
2. L. L. Kesmodel and L. M. Falicov, Solid State Comm., 16, 1201 (1975).
3. M. A. Chesters and G. A. Somorjai, Surf. Sci., 52, 21 (1975).
4. G. T. Grant, Surf. Sci., 25, 451 (1971).
5. H. Conrad, G. Ertl, J. Koch, and E. E. Latta, Surf. Sci., 43, 462 (1974).
6. K. Klier, A. C. Zettlemoyer, and H. Leidheiser, J. Chem. Phys., 52, 589 (1970).
7. K. Christmann and G. Ertl, Z. Naturforsch., 28a, 1144 (1973).
8. V. N. Ageev and N. I. Ionov, Zh. Tekh. Fiz., 41, 2196 (1971).
9. M. A. Fortes and B. Ralph, Proc. Roy. Soc. A, 307, 431 (1968).
10. H. Conrad, G. Ertl, and E. E. Latta, Surf. Sci., 41, 435 (1974).
11. B. Lang, R. W. Joyner, and G. A. Somorjai, Surf. Sci., 30, 454 (1972).
12. J. A. Joebstl, J. Vac. Sci. Tech., 12, 347 (1975).
13. D. B. Rogers, R. D. Shannon, A. W. Sleight, and J. L. Gillson, Inorg. Chem., 8, 841 (1969).
14. A. E. Morgan and G. A. Somorjai, J. Chem. Phys., 51, 3309 (1969).
15. R. L. Palmer and J. N. Smith, J. Chem. Phys., 60, 1453 (1974).

FIGURE CAPTIONS

- Fig. 1. LEED patterns of CO adsorbed on Ir(111)
(a) clean Ir(111) at 71 V, (b) $(\sqrt{3}\times\sqrt{3})R$ 30°-CO at 70 V, and
(c) $(2\sqrt{3}\times2\sqrt{3})R$ 30°-CO at 75 V.
- Fig. 2. Models proposed for
(a) $(\sqrt{3}\times\sqrt{3})R$ 30°-CO and (b) $(2\sqrt{3}\times2\sqrt{3})R$ 30°-CO surface structures.
Indicated are the unit meshes of the adsorbed layer (in dashed lines) and of the substrate (in full lines).
- Fig. 3. Thermal desorption of CO from Ir(111) (Fig. 3a) and
Ir(S)-[6(111) \times (100)] (Fig. 3b). The heating rates used are
about 25 degrees/sec for both faces.
- Fig. 4. The amount of CO adsorbed on Ir(111) versus exposure as derived from
thermal desorption and AES measurements. Indicated are two values
of the coverage θ (defined as equal to 1 when the number of adsorbed
CO molecules equals the number of metal atoms on the surface.).
- Fig. 5. An adsorption isostere for CO on Ir(111) for a relative coverage
near 1/3.
- Fig. 6. The Auger spectrum near the carbon peak for
(a) clean Ir, (b) amorphous C on Ir, and (c) CO adsorbed on Ir(111).
- Fig. 7. LEED patterns of oxygen adsorbed on Ir(111). Electron energy 80 V.
(a) at an exposure of about 10 L and (b) at an exposure of about 30 L.
- Fig. 8. Thermal desorption spectra for oxygen adsorbed on Ir(111). The
heating rate was about 70 degrees/sec.
- Fig. 9. The amount of oxygen adsorbed at room temperature on Ir(111) as a
function of exposure.
- from the height of the oxygen Auger 520 eV transition
 - from thermal desorption.

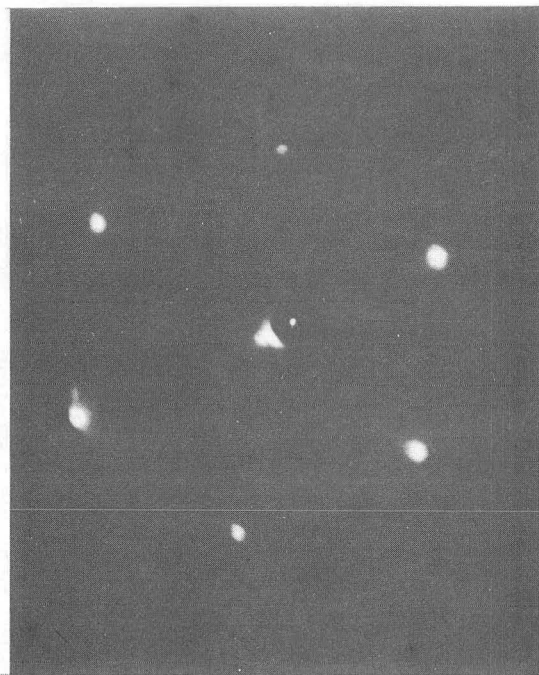
Fig. Cap., contd.

Fig. 10. LEED patterns of oxygen adsorbed on Ir(S)-[(111)×(100)]
(a) clean Ir(S)-[6(111)×(100)], (b) (2×2)-0 surface structure,
(c) (2×1)-0 surface structure with an initial development of
streaks perpendicular to the steps. (d) after heating (c) in
 10^{-7} Torr O₂ above 450°C.

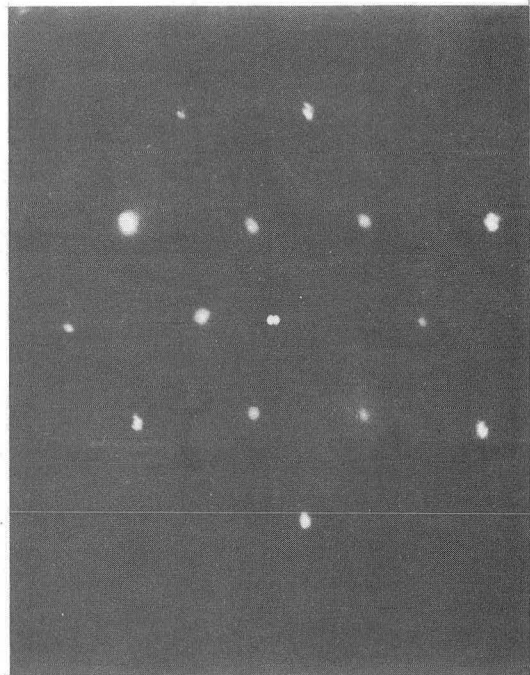
All pictures were taken at 110 V.

Fig. 11. Thermal desorption spectra of oxygen from Ir(S)-[6(111)×(100)].
Heating rate is approximately 100 degrees/sec.

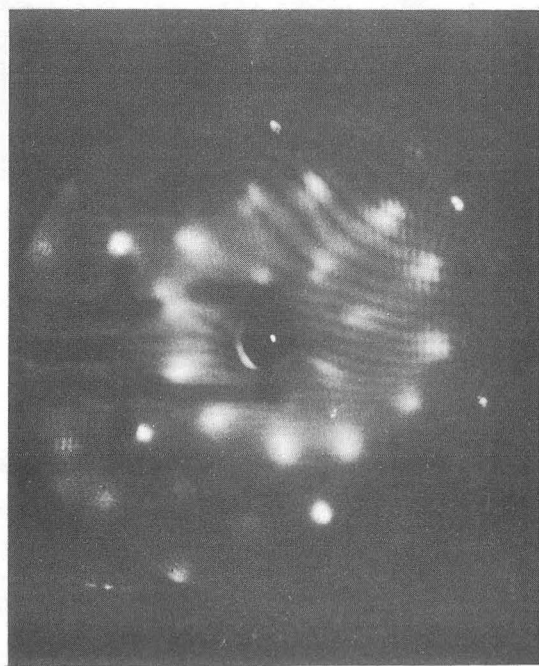
Fig. 12. Increase in CO₂ pressure when the Ir(111) interface is exposed to
a 1:1 mixture of CO and CO₂.



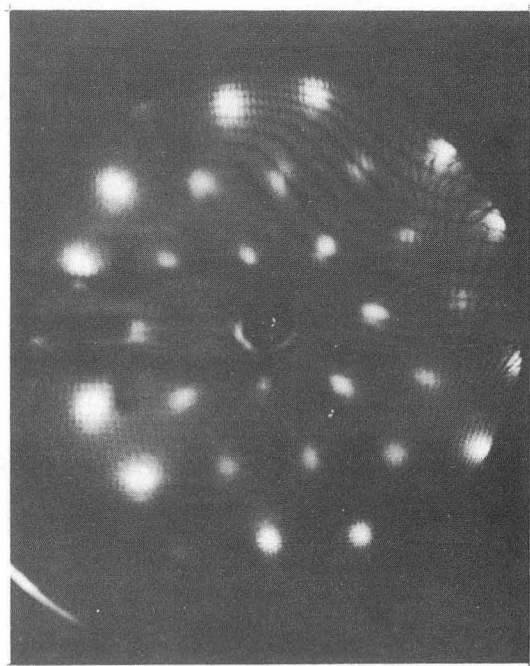
a



b



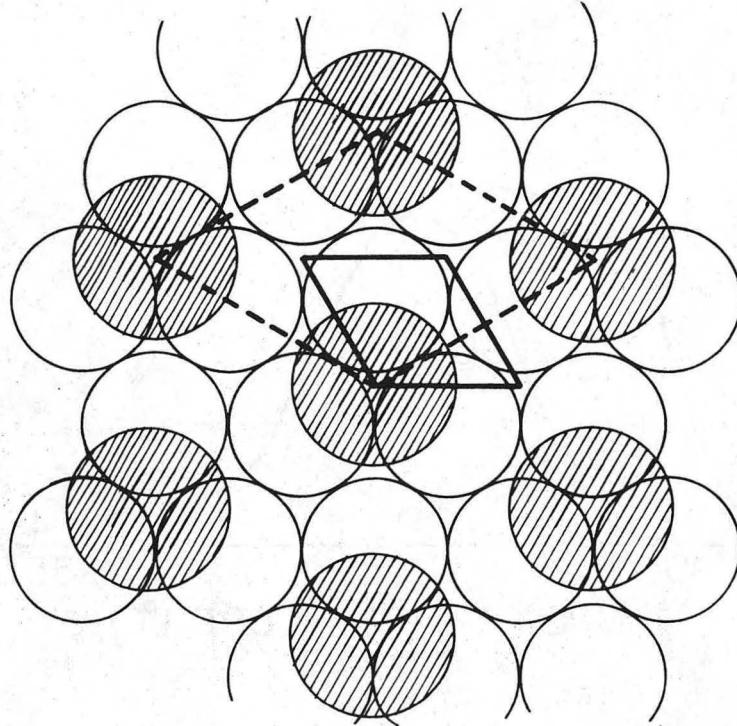
c



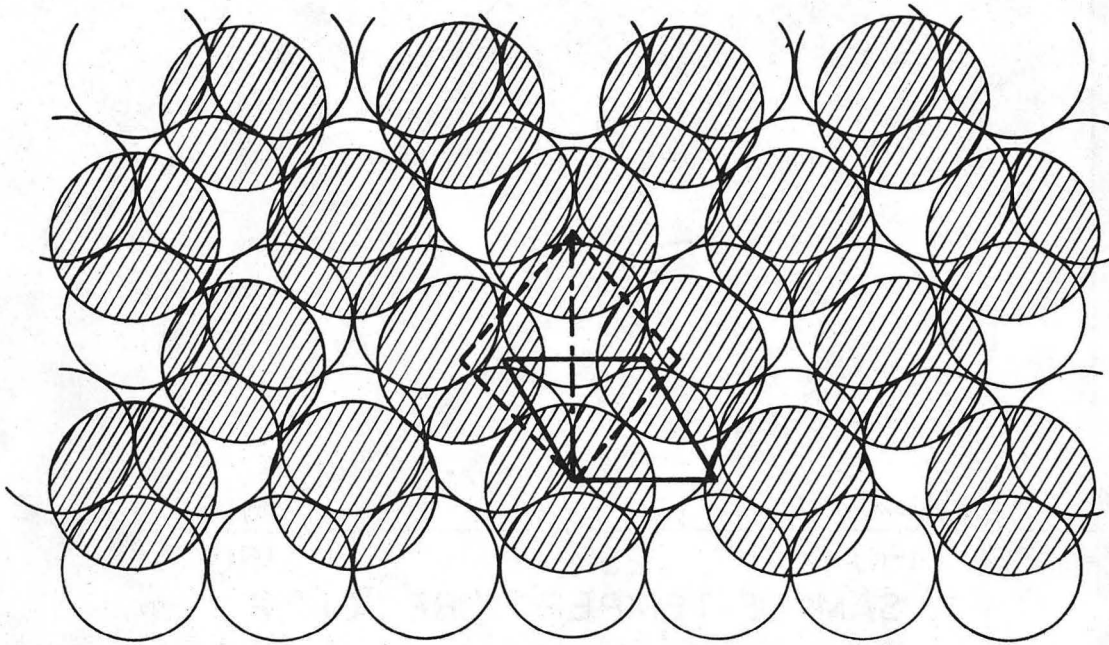
d

XBB 7510-7797

Figure 1
a,b,c,d



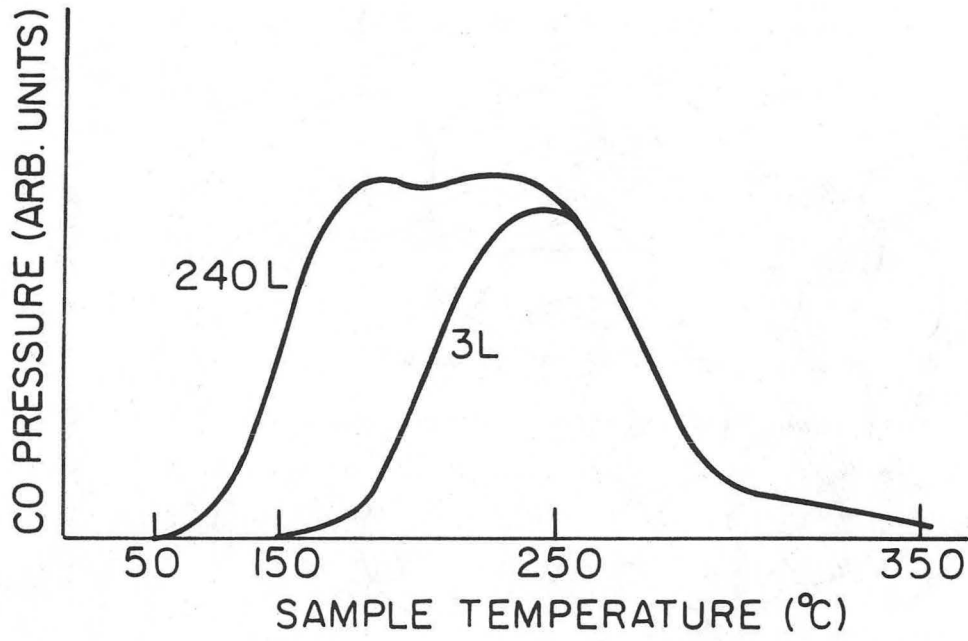
(a)



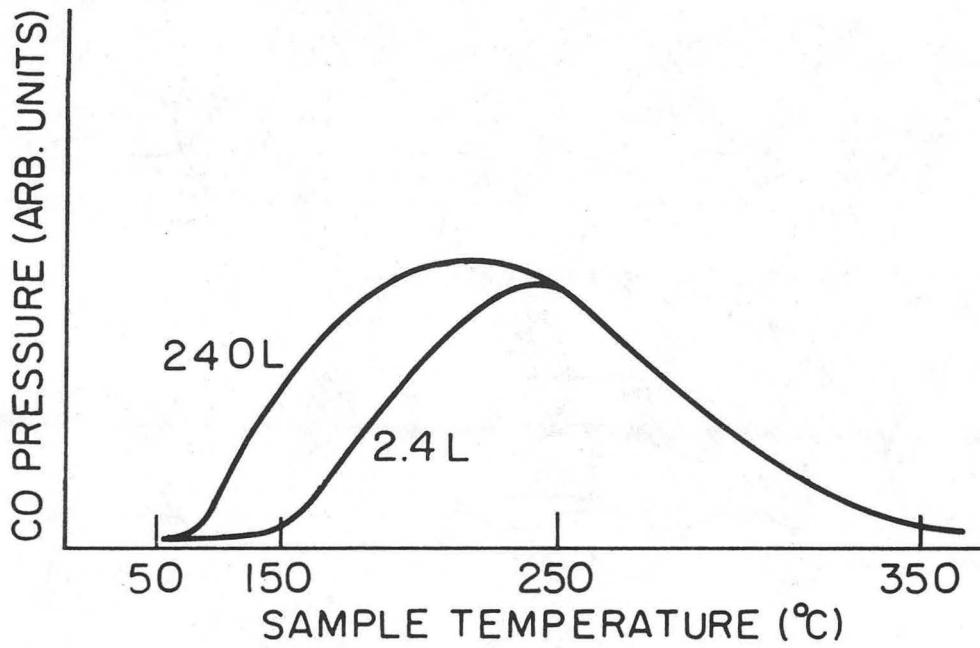
(b)

XBL7510-7542

Figure 2
a,b



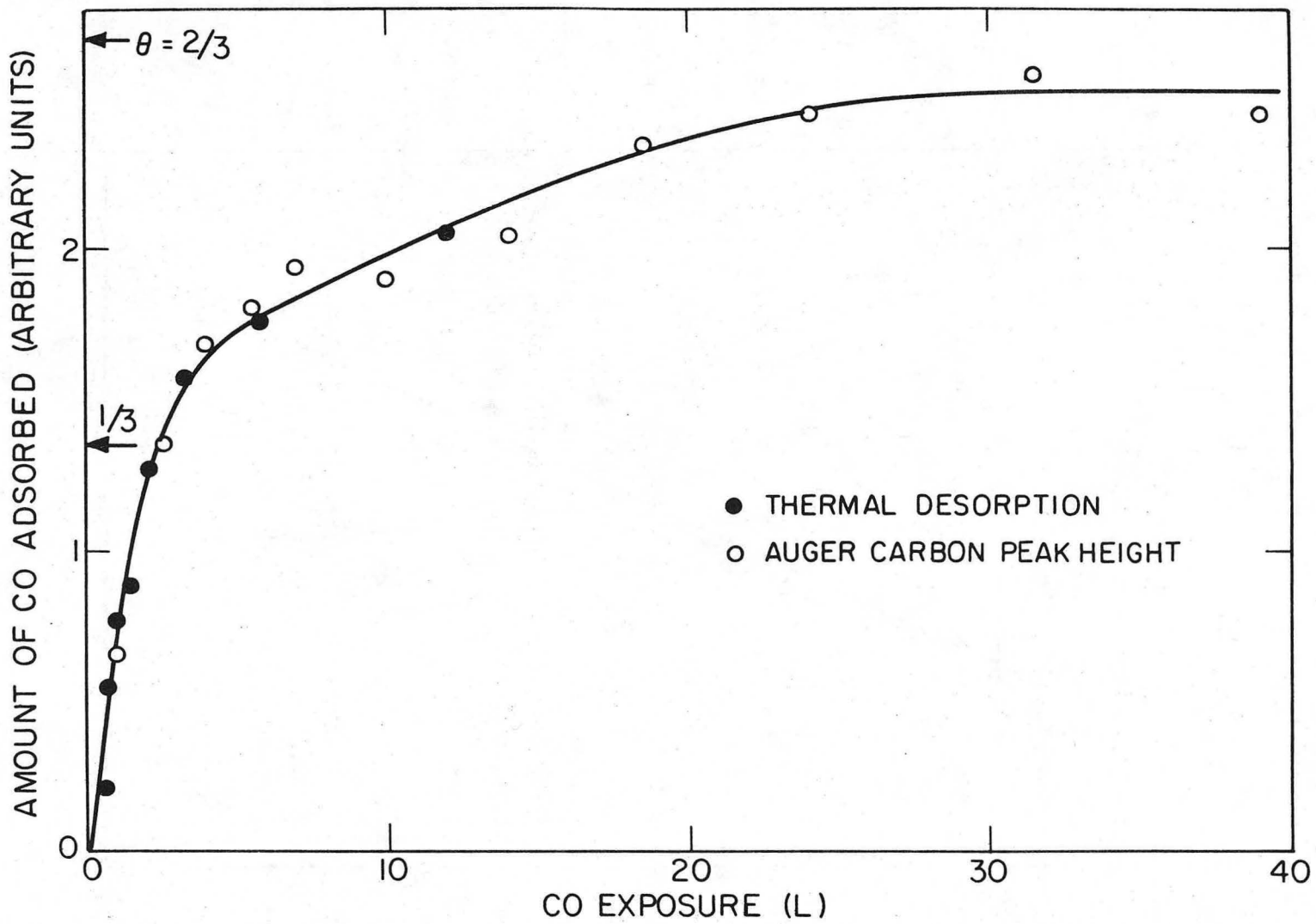
(a)



(b)

XBL 7510-7543

Figure 3
a,b



XBL7510-7544

Figure 4

00004407052

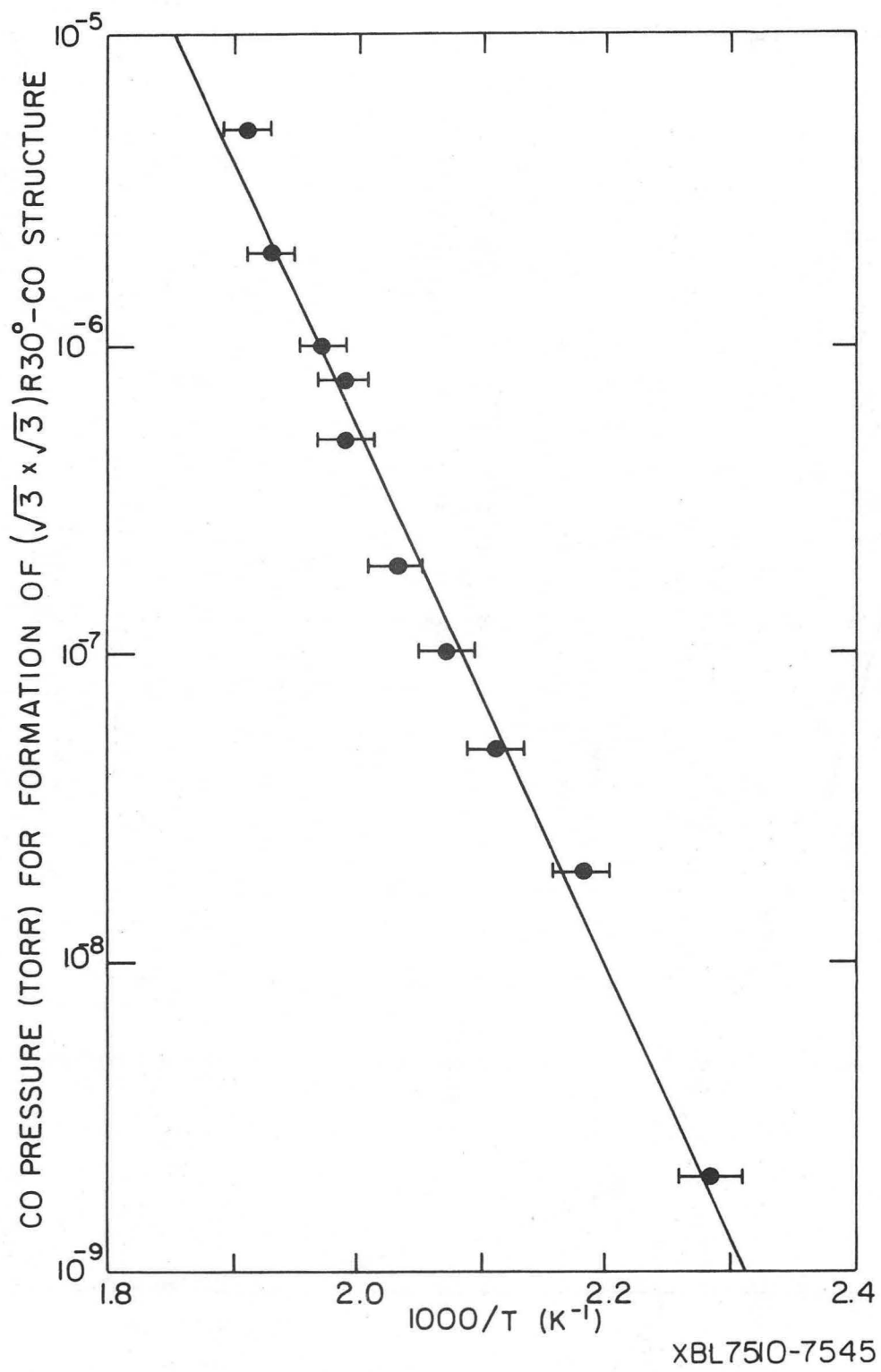
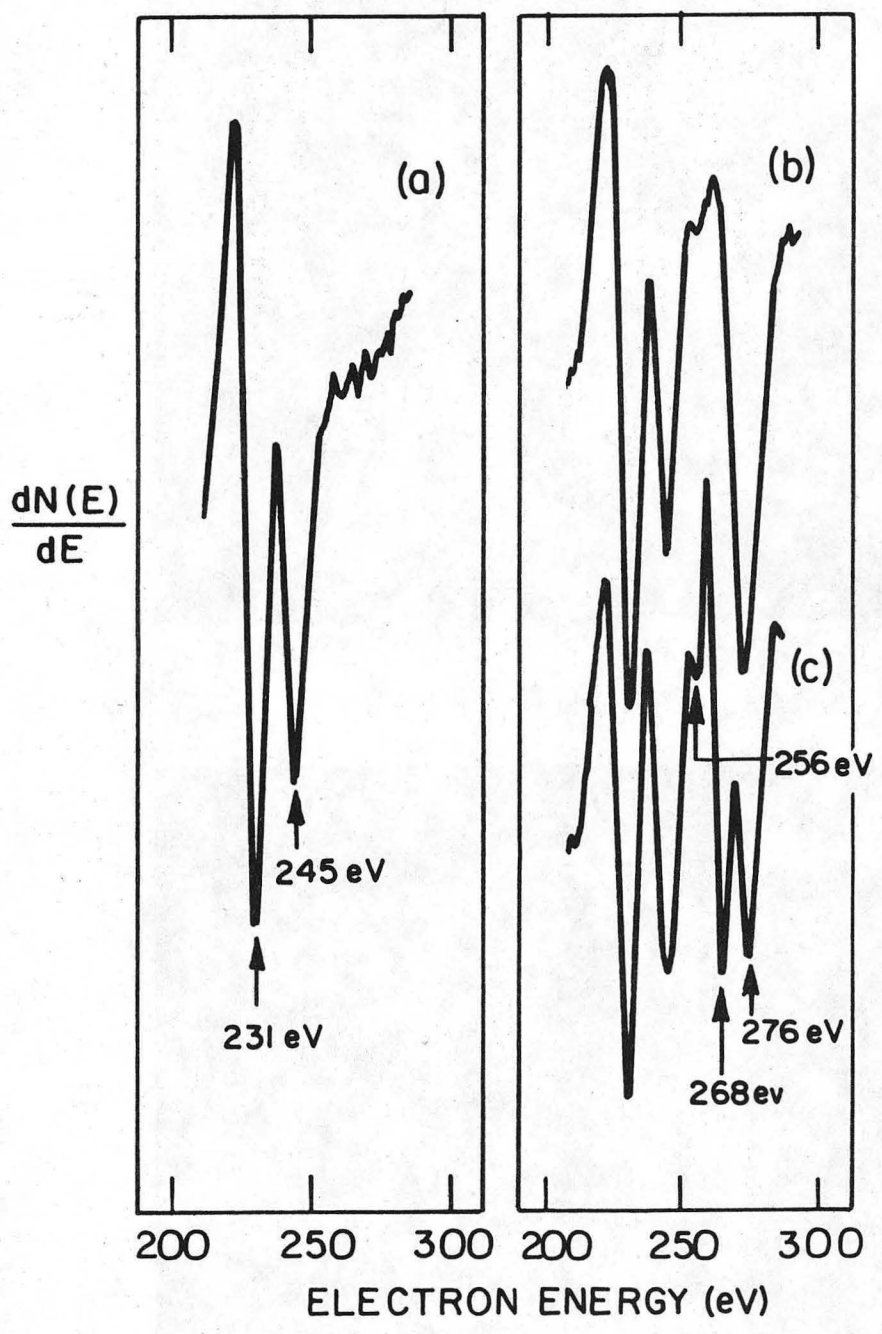
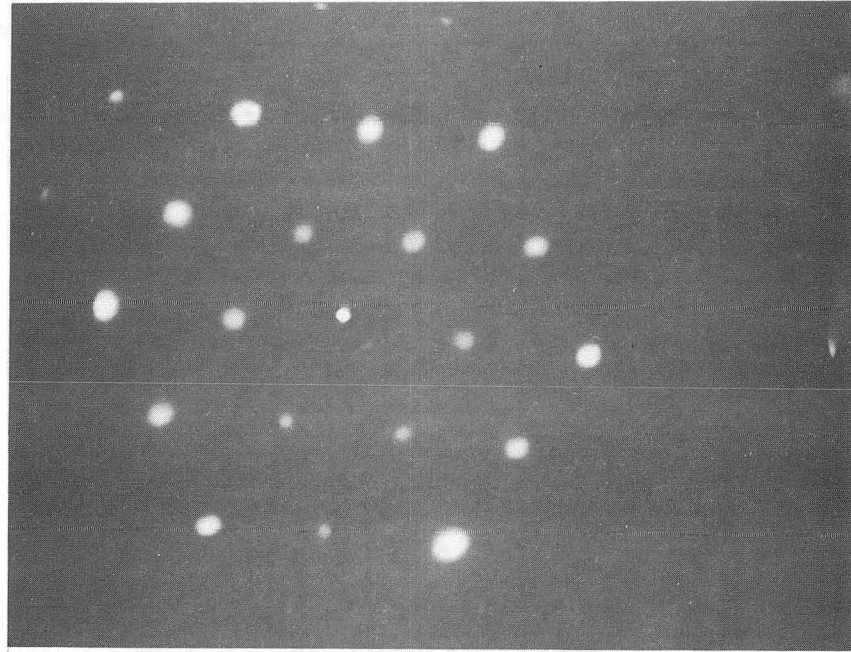


Figure 5

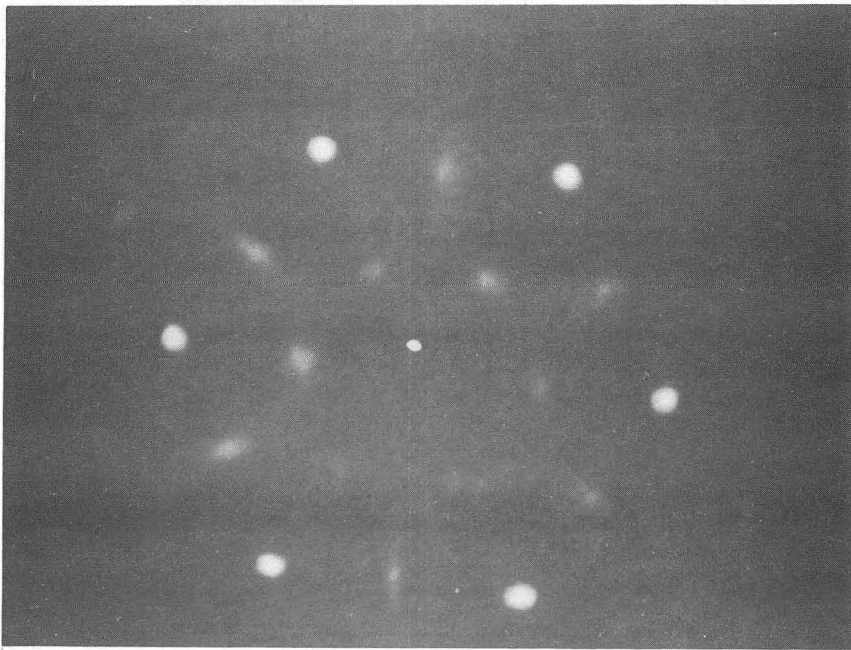


XBL7510-7546

Figure 6



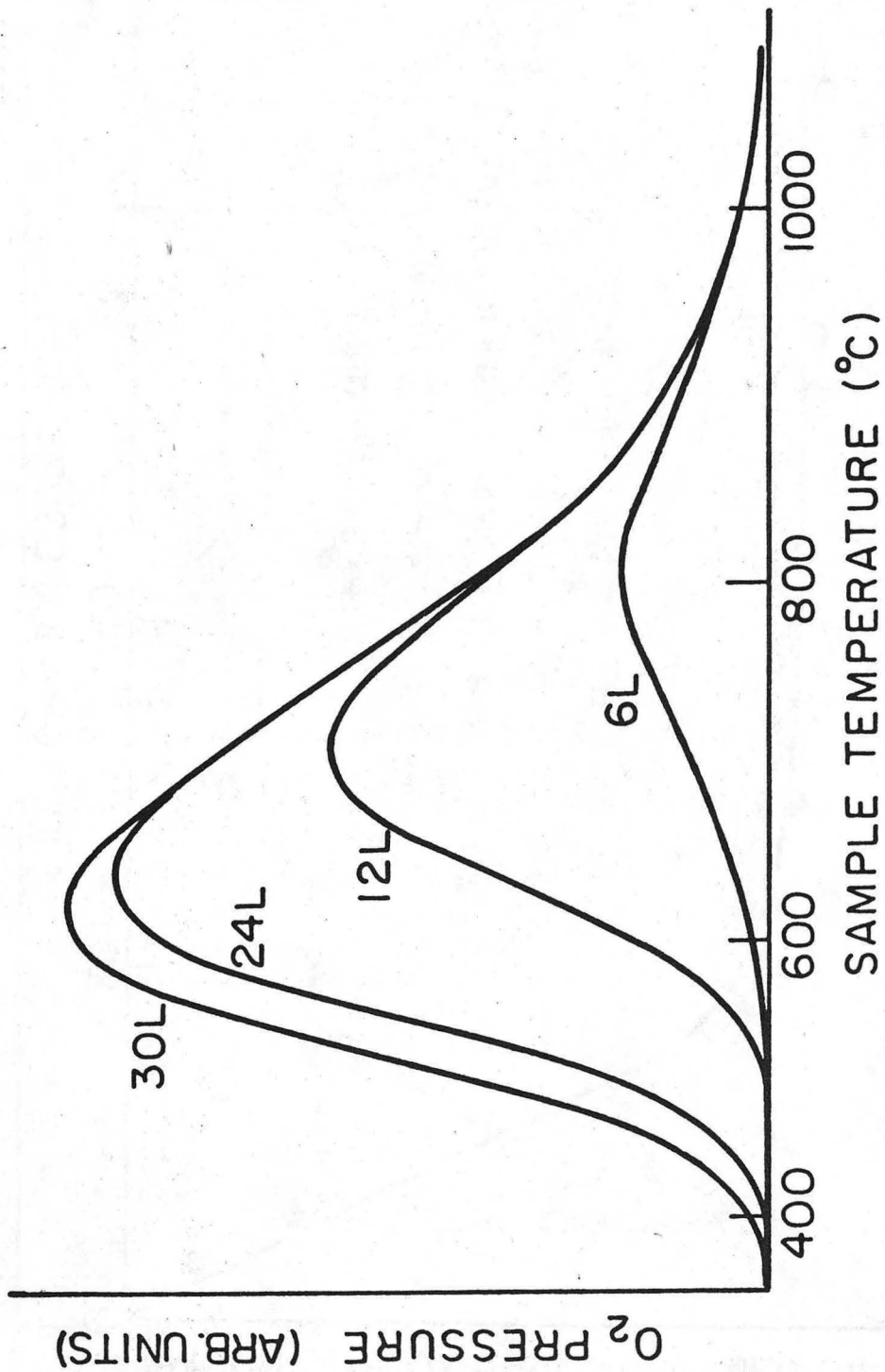
a



b

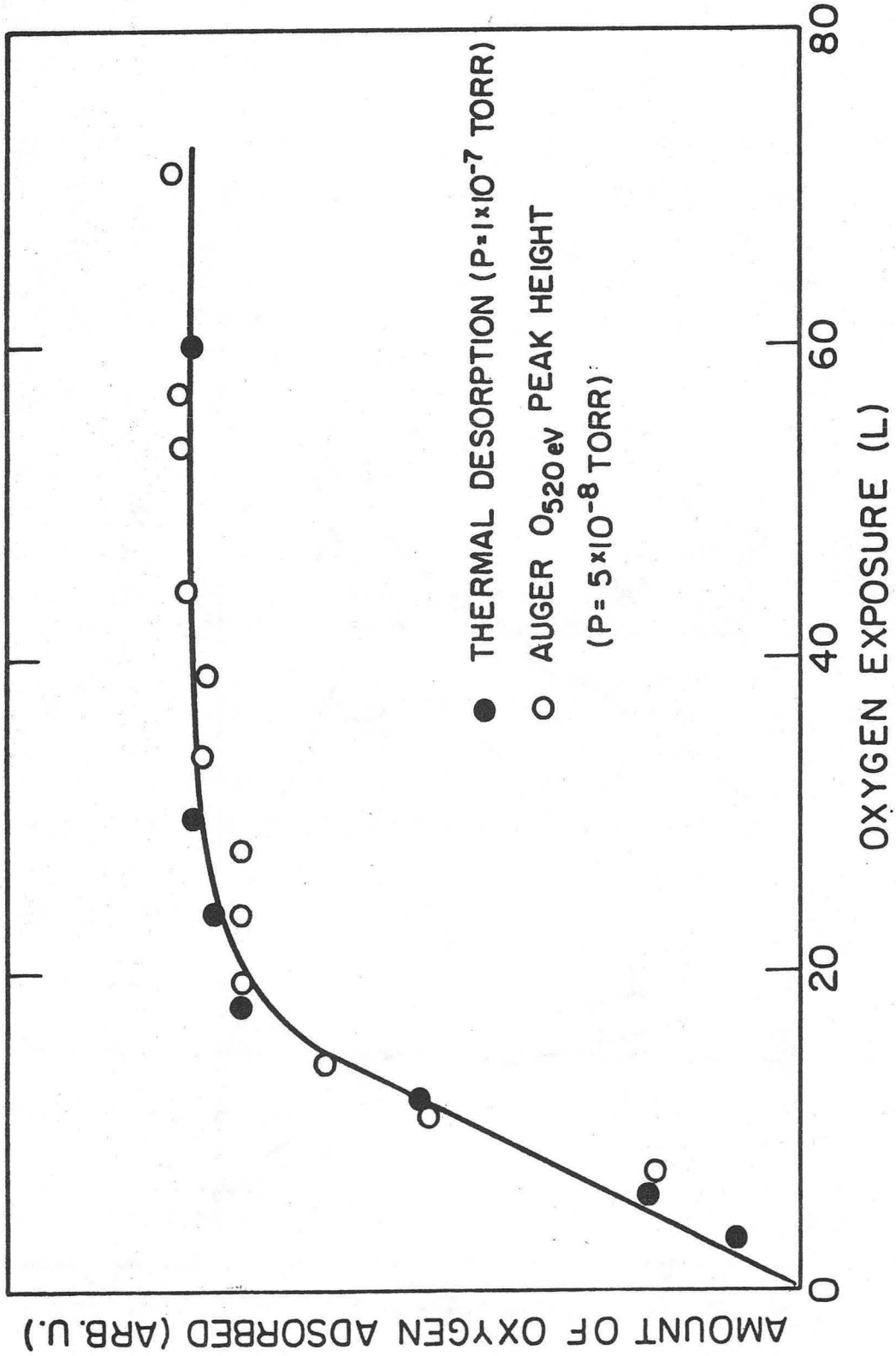
XBB 7510-7799

Figure 7
a,b



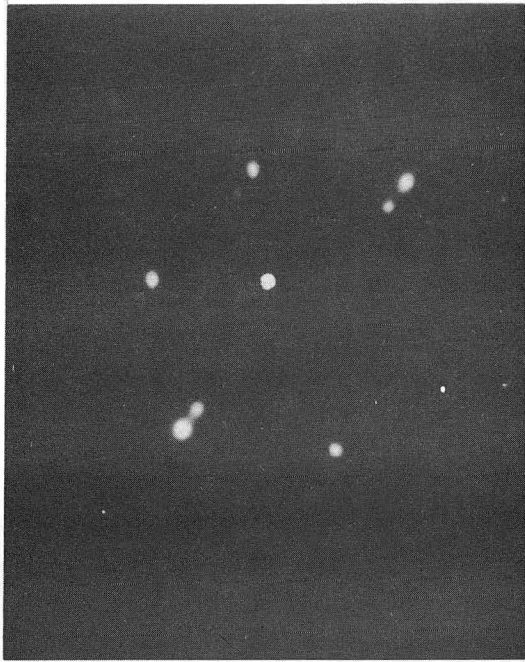
XBL7510-7547

Figure 8

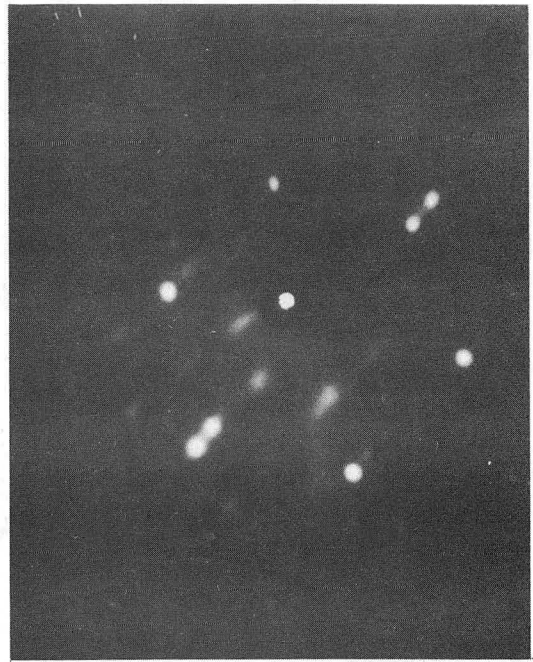


XBL 7510-7548

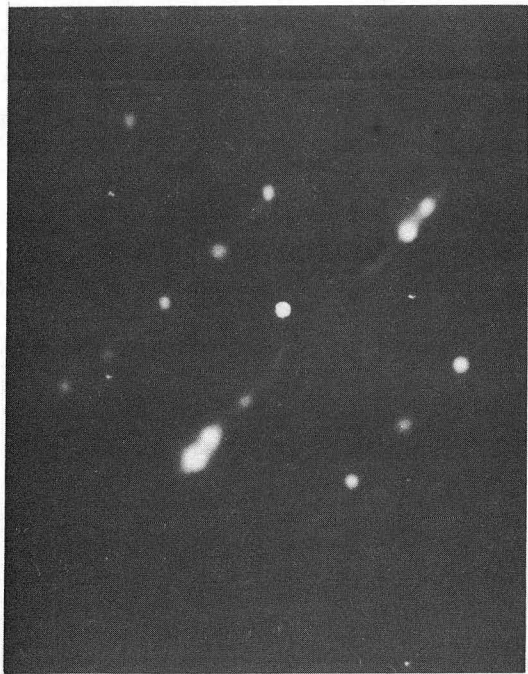
Figure 9



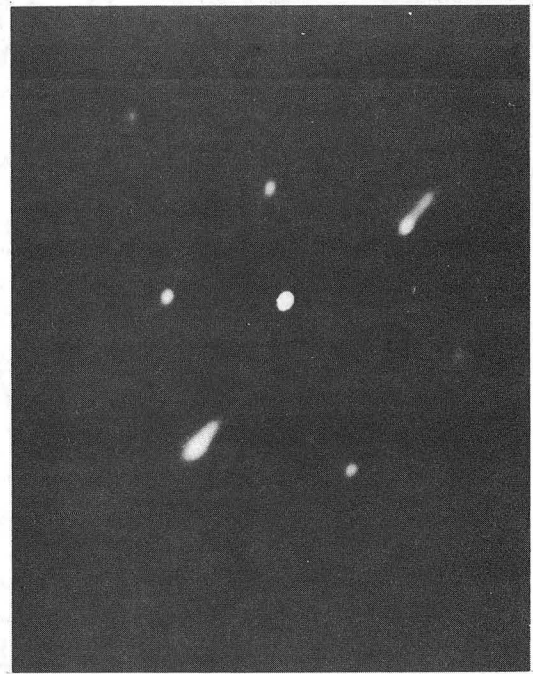
a



b



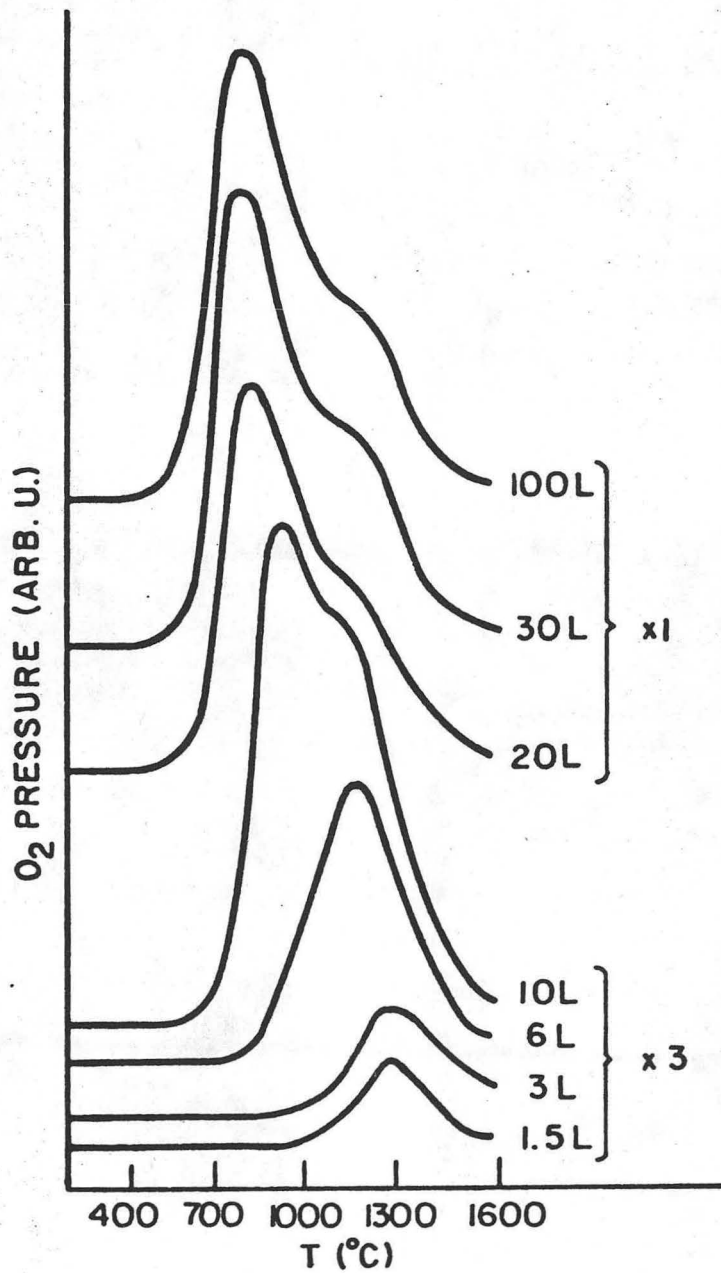
c



d

XBB 7510-7798

Figure 10
a,b,c,d



XBL 7510-7549

Figure 11

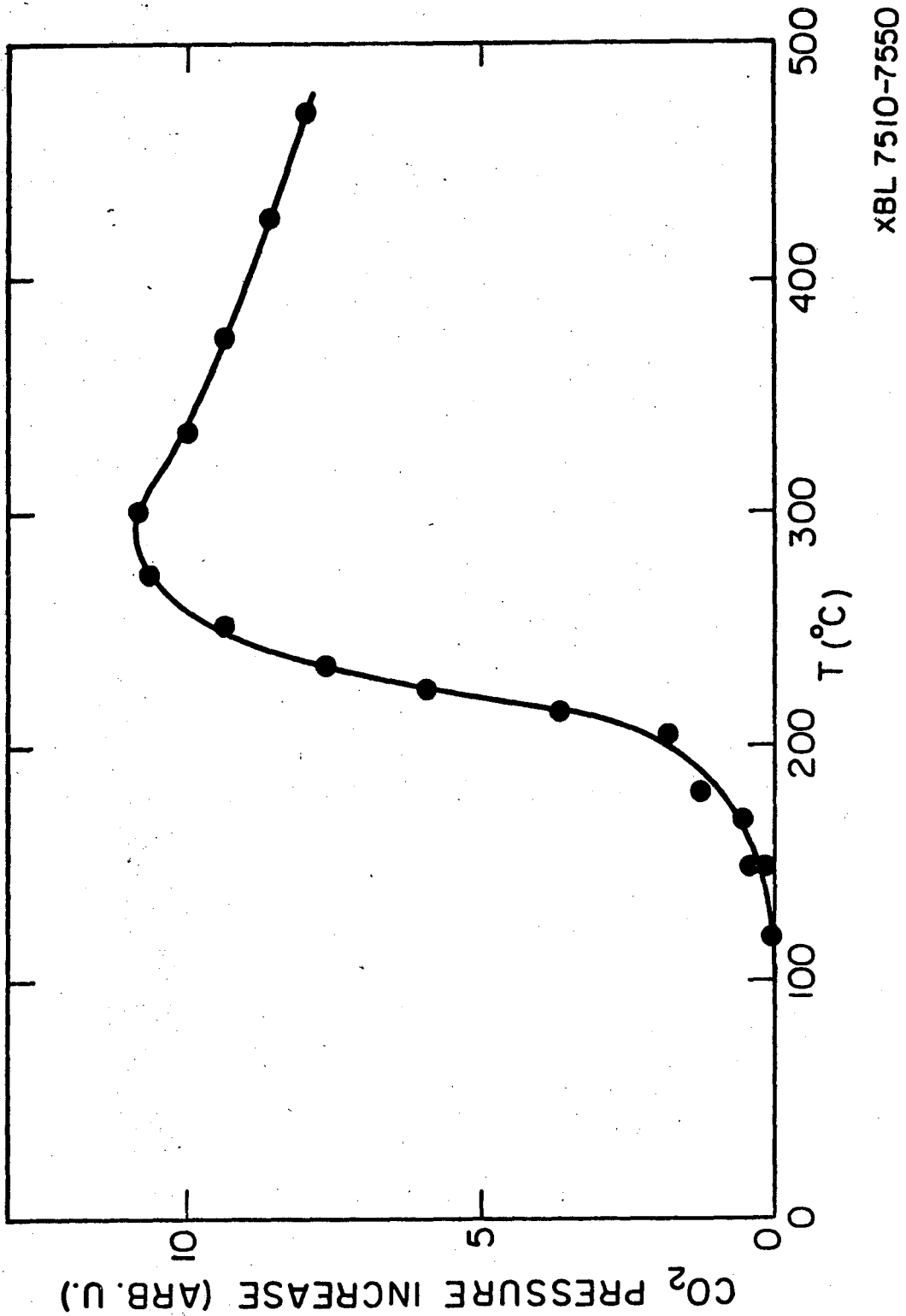


Figure 12

LEGAL NOTICE

This report was prepared as an account of work sponsored by the United States Government. Neither the United States nor the United States Energy Research and Development Administration, nor any of their employees, nor any of their contractors, subcontractors, or their employees, makes any warranty, express or implied, or assumes any legal liability or responsibility for the accuracy, completeness or usefulness of any information, apparatus, product or process disclosed, or represents that its use would not infringe privately owned rights.

TECHNICAL INFORMATION DIVISION
LAWRENCE BERKELEY LABORATORY
UNIVERSITY OF CALIFORNIA
BERKELEY, CALIFORNIA 94720